LASER INTERFEROMETER GRAVITATIONAL WAVE OBSERVATORY
- LIGO -
CALIFORNIA INSTITUTE OF TECHNOLOGY
MASSACHUSETTS INSTITUTE OF TECHNOLOGY

| **Technical Note** | **LIGO-T22xxxxx–** | 2026/07/31 |
|---|---|---|

# Optical Enhancement Cavity Project Interim Report 2

Jack Ryan

**California Institute of Technology**
**LIGO Project, MC100-36**
**Pasadena, CA 91125**
Phone (626) 395-2129
Fax (626) 304-9834
E-mail: info@ligo.caltech.edu

**Massachusetts Institute of Technology**
**LIGO Project, Room NW22-295**
**Cambridge, MA 02139**
Phone (617) 253-4824
Fax (617) 253-7014
E-mail: info@ligo.mit.edu

**LIGO Hanford Observatory**
**Route 10, Mile Marker 2**
**Richland, WA 99352**
Phone (509) 372-8106
Fax (509) 372-8137
E-mail: info@ligo.caltech.edu

**LIGO Livingston Observatory**
**19100 LIGO Lane**
**Livingston, LA 70754**
Phone (225) 686-3100
Fax (225) 686-7189
E-mail: info@ligo.caltech.edu

http://www.ligo.caltech.edu/

# Contents

**1 Introduction** **2**

**2 Background** **2**

**3 Project Objectives** **4**

**4 Previous Work** **5**

**5 Progress** **7**

5.1 PDH Lock . . . . . 7

5.2 Cavity Ring Down Measurement . . . . . 10

5.3 Challenges . . . . . 12

**6 Future Steps** **12**

# 1 Introduction

The Laser Interferometer Gravitational-wave Observatory (LIGO), utilizes long baseline Michelson interferometers to detect gravitational waves (GWs) generated by astronomical events like black hole mergers or neutron star collisions. As GWs pass through each detector, they warp space-time, changing the path-length difference of the Michelson interferometers leading to a detectable signal. In order to enhance this signal, LIGO makes use of Fabry-Perot cavities to increase the power within each arm of the interferometer. This increased power enhances the modulation GWs cause, increasing the sensitivity of the detector [1]. This principle of utilizing optical cavities to build up high amounts of optical power has broad applications across physics, including in laser inertial confinement fusion.

Blue Laser Fusion (BLF) is working to establish the world's first inertial fusion energy (IFE) generation. BLF utilizes Coherent Beam Combining (CBC) technology and an Optical Enhancement Cavity (OEC) to produce a highly efficient pulsed laser system capable of producing 10 kJ pulses at repetition rates of 1 to 10 Hz. Through the combination of 500 of these systems, BLF aims to generate 5 MJ pulses at high repetition rates for fusion ignition [2].

The focus of this project will be on the OEC. An OEC is a Fabry-Perot optical cavity capable of building up and storing high intracavity powers. Past work on the OEC has achieved enhancement of a continuous wave (CW) laser beam by a factor of 58,461, achieving circulating powers of several kW within a 1.5 m demonstration cavity [3]. A key next step for the OEC, however, is achieving locking to the OEC with the laser operating in pulsed mode. Pulsed operation of the OEC allows for high peak powers required for inertial fusion, but introduces significant challenges.

This project aims to demonstrate pulse-locking of our laser to the OEC and to understand the technical challenges of locking pulses to a high finesse optical cavity. The techniques utilized can be adapted to 15 m and 150 m enhancement cavities currently in development at BLF for the purpose of fusion.

# 2 Background

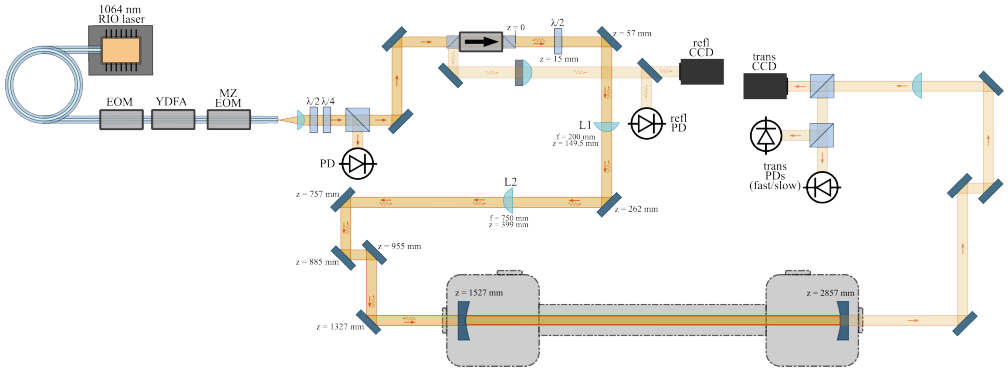



Figure 1: Schematic of current OEC setup. Figure credit: Georgia Bolingbroke

The OEC is a standard Fabry-Perot optical cavity consisting of two highly reflective mirrors. Light directed into the cavity that satisfies the resonant condition

$$n\lambda = 2L \tag{1}$$

where $\lambda$ is the wavelength of incident light, L is the length of the cavity, and n is an integer, builds up over time as the accumulated phase of circulating light matches new incident light, constructively interfering.

Related to this resonance condition is the free spectral range (FSR) of the cavity, which is a measure of the distance between resonant peaks of the cavity in the frequency domain. By substituting $c/f = \lambda$ into Eq. 1, we see that the distance between resonant peaks is given by

$$FSR = \frac{nc}{2L} \tag{2}$$

with resonant peaks contained at an integer multiple of the FSR.

A measure of how well light is stored in the cavity is called the finesse, measuring the average number of times a photon circulates before it exits the cavity. The OEC is a cavity with ultra-high finesse, with mirror losses of only 3.4 parts-per-million (ppm). This ultra-high reflectivity yields a theoretical finesse given by

$$Finesse \approx \frac{\pi(R_1R_2)^{1/4}}{1-(R_1R_2)^{1/2}} \tag{3}$$

where R is the reflectivity of the mirrors. If the losses in our cavity are only derived from transmission through the mirrors, the theoretical finesse of the OEC is approximately 924,000. In practice, the finesse will be lower than this value as intracavity losses occur due to stray dust and imperfect alignment.

To minimize these losses, the OEC is contained within an ultra-high-vacuum (UHV) chamber reaching pressures of $10^{-9}$ torr. Prior to this project, significant work with the OEC has already been completed as summarized in Ref. [3]. Through this work, the OEC achieved a finesse of 419,000.

The FSR and finesse of the cavity are related through the relation

$$Finesse = \frac{FSR}{\Delta\nu} \tag{4}$$

where $\Delta\nu$ is the linewidth of the cavity's resonant condition. Using the estimated finesse and FSR of the OEC, the linewidth of the cavity is approximately 250 Hz. This extremely narrow linewidth necessitates the usage of feedback to keep the laser locked to the cavity, which will be covered in depth in the methods section.

A last key concept relating to the OEC is mode matching. When coupling the input laser beam, which has a Gaussian profile, into the optical cavity, only a certain set of transverse electromagnetic (TEM) modes, are allowed by boundary conditions [4]. To efficiently couple

power into the cavity, we want to match the incoming beam shape to the fundamental $\mathrm{TEM}_{00}$ mode, avoiding excess power into higher order modes (HOMs).

To mode match, the beam's Gaussian shape described by the q-parameter

$$q(z) = z + iz_R, \qquad z_R = \frac{\pi w_0^2}{\lambda}, \tag{5}$$

where $w_0$ is the beam waist, $z$ the distance, $z_R$ the Rayleigh range, and $\lambda$ the wavelength, is shaped utilizing lenses to spatially match the cavity's $\mathrm{TEM}_{0,0}$ eigenmode at the input mirror. To find the shape of the $\mathrm{TEM}_{0,0}$ eigenmode, ABCD matrices are utilized.

Within an optical system, the propagation of a Gaussian beam can be described by ABCD matrices, with optical components such as mirrors, beam splitters, and lenses having unique transfer matrices, covered in Ref. [4].

To find the $\mathrm{TEM}_{0,0}$ eigenmode of the optical cavity, we require that the mode must reproduce itself after each round trip. This gives the condition

$$q_{cav} = q_1 = \frac{Aq_1 + B}{Cq_1 + D}. \tag{6}$$

Which can be rearranged to give the following quadratic equation

$$Cq_{cav}^2 + (D - A)q_{cav} - B = 0 \tag{7}$$

By solving this equation, we can solve for $q_{cav}$, and find the eigenmode's waist size, location, and spot size at the input mirror. Once these parameters are known, a mode matching solution utilizing two to three lenses is found to match the beam's q-parameter to $q_{cav}$ as closely as possible, maximizing the circulating power into the cavity [4].

# 3 Project Objectives

The primary objective of this project is to demonstrate pulse locking of the laser to the OEC. Prior work with the OEC has achieved stable locking to an ultra-high-finesse cavity with the laser operating as a continous wave (CW), however, additional challenges arise when attempting to lock the cavity with a pulsed laser [3]. This is because in order for a coherent build up of optical pulses to occur, the FSR must precisely match the pulse rate of the laser. Additional challenges also arise when attempting to maintain a stable lock to the cavity with a pulsed laser, as you no longer have a continuous signal for the locking loop. Addressing and overcoming these challenges will be an integral part of this project, and the techniques developed and learned will be utilized within BLF's larger 15 m and 150 m cavities. To achieve the larger objective of pulse locking, this project seeks to achieve several smaller goals outlined below:

**Integrate new mirrors and realign cavity**

A new set of 3.4 ppm loss mirrors have been delivered for usage in the OEC. The first objective of this project is to implement these new mirrors, and to realign the cavity with a new mode matching solution implemented.

**Achieve a stable continous wave lock to the OEC**

After the OEC has been realigned, we will reestablish a stable lock to the cavity's $TEM_{0,0}$ mode through a Pound-Drever-Hall (PDH) lock.

**Characterize pulse shape**

Once the cavity has been aligned and locked, we will begin to characterize the pulsed laser. This will include understanding the temporal pulse shape, bandwidth, and electronics involved in generating and observing the pulses.

**Perform pulse locking on OEC**

Once the pulses have been characterized, we will lock the pulsed laser to the OEC by dithering, or slowly varying the laser. If time permits, we will also investigate an improved form of locking through balanced homodyne readout.

**Analyze results and address limitations**

Since the OEC is a demonstration cavity, a key objective is to understand and interpret the procedure, limitations, and effectiveness of pulse locking to the cavity. The techniques we use and develop can then be adapted to the larger BLF cavities in development.

# 4 Previous Work

During the first week of this project, I gained familiarity with the cavity setup with simulations through the Finesse Python package. In Finesse, I modeled the OEC and the expected error signal derived for the PDH lock, as well as the generation of higher order modes from cavity misalignment. I also read several papers in relation to cavity mode matching and the ABCD matrix formulation for optics.

During the second week the new set of cavity mirrors with 3.4 ppm loss and radius of curvature of 15 m were installed. Because of this new setup, a new alignment for the cavity as well as a new mode matching solution was required. The cavity was aligned by carefully steering the beam with the external mirrors until we visualized a clean $TEM_{00}$ mode on the transmitted and reflected CCD cameras. The aligned beam path was marked with a set of 5 irises for future realignment.

I then profiled the laser beam to obtain the waist location and waist quadrature measurements necessary for obtaining a new mode matching solution for the cavity. To profile the beam, a WinCamD beam profiler was set in the beam path after the Faraday isolator (FI), where z=0 denotes the edge of the FI shown in Fig. 1. DataRay software was utilized to take a set of 5 waist measurements as I moved the profiler 5-10 mm at a time in reference to a ruler. The waist versus distance data was then imported into Python to fit the data to the waist equation given by

$$w(z) = w_0\sqrt{1 + (\frac{z}{z_R})^2} \tag{8}$$

where w(z) is the waist as a function of distance, and $z_R$ is the Rayleigh range. Utilizing Scipy curvefit, the following fit was found from the data:

X(u): $w_0$ = 60.26 +/- 0.21 um, z0 = -45.30 +/- 0.43 mm, $z_R$ = 10.72

Y(v): $w_0$ = 61.07 +/- 0.14 um, z0 = -46.74 +/- 0.30 mm, $z_R$ = 11.01

The fit versus distance along with the residuals is shown below in Fig. 2.

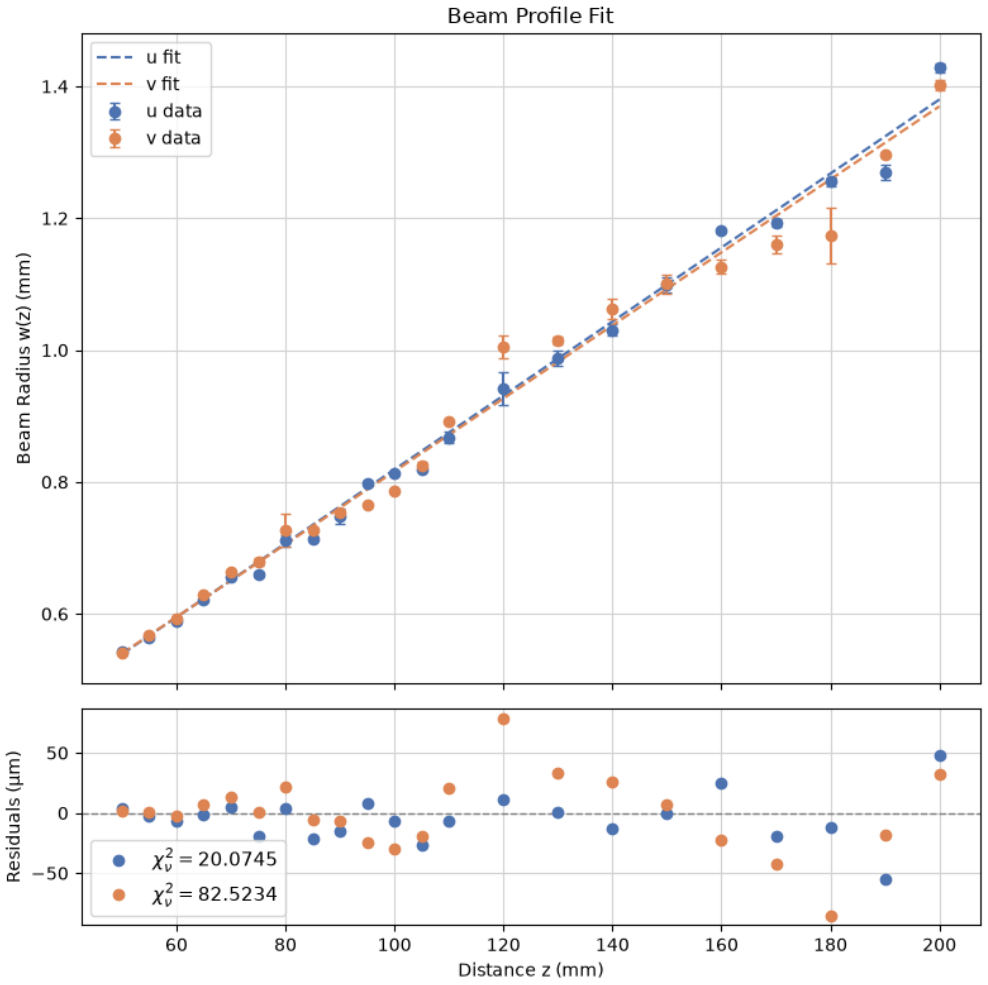



Figure 2: Gaussian beam fit (top) and residuals of fit (bottom).

After profiling the beam, the waist, waist position (z0), and Rayleigh range were utilized by Peter Carney to compute a new mode matching solution for the cavity following methods discussed in the background section.

The solution found consisted of two lens, Lens 1 at z=149.5 mm after the FI with focal length of 0.200 m, and Lens 2 at 399.4 mm after the FI with focal length of 0.750 m. The lens and their locations are showcased in Fig. 1. After implementing the lens, the beam was aligned to the cavity by steering through all 5 irises.

With the beam coarsely aligned through the irises to the cavity, the transmitted CCD camera was used to visualize the cavity's modes. An aligned cavity will showcase a strong $TEM_{00}$

mode, with little to no HOMs present. HOMs were initially present indicating misalignment of the beam. The beam was finely walked and the lenses translated with a linear stage until a strong $TEM_{00}$ peak was observed.

At this stage, we have implemented a new set of highly reflective mirrors, reprofiled the beam, found a corresponding mode matching solution, and realigned the cavity. Our next steps are to lock the cavity to the $TEM_{00}$ mode utilizing the PDH procedure. After this, we can measure the FSR of the cavity, and proceed with pulse locking of the laser.

# 5 Progress

## 5.1 PDH Lock

After aligning the cavity, the next step was to achieve a stable lock of the OEC through the Pound–Drever–Hall (PDH) method covered in depth by Black in Ref. [5]. The PDH method allows for the power observed at the reflection photodetector to be converted into an error signal that can be utilized to tune the laser towards the cavity's resonance.

The first step to performing a PDH lock to the OEC was to use a fiber coupled Electro-Optic Modulator (EOM) to generate frequency sidebands of the laser. Following Black's notation, phase modulation of the beam at frequency $\Omega$ produces a carrier and two sidebands above and below the carrier frequency [5], given by

$$E_{\text{inc}} \approx E_0 \left[ J_0(\beta)\, e^{i\omega t} + J_1(\beta)\, e^{i(\omega+\Omega)t} - J_1(\beta)\, e^{i(\omega-\Omega)t} \right] \tag{9}$$

where $\beta$ is the modulation depth and $J_n$ are Bessel functions. The carrier power is $P_c = J_0^2(\beta)P_0$ and the power in each first-order sideband is $P_s = J_1^2(\beta)P_0$, with $P_0$ the total incident power.

This modulated light is then directed into the OEC, where the sidebands are off resonance and promptly reflect at the input mirror, while the carrier light enters the cavity, acquiring a phase shift before it leaks out. Each frequency component is reflected according to the cavity's reflection coefficient, given by

$$F(\omega) = \frac{E_{\text{refl}}}{E_{\text{inc}}} = \frac{r\left(\exp\left(i\dfrac{\omega}{\Delta\nu_{\text{fsr}}}\right) - 1\right)}{1 - r^2 \exp\left(i\dfrac{\omega}{\Delta\nu_{\text{fsr}}}\right)} \tag{10}$$

where $r$ is the amplitude reflection coefficient of the cavity mirrors and $\Delta\nu_{\text{fsr}}$ the free spectral range. The combination of the carrier's leakage light and the promptly reflected sidebands is then directed onto the reflection PD.

The power incident on the reflection PD is the sum of the reflected carrier and the sidebands, given by Black's Eq. (3.3) as

$$
\begin{aligned}
P_{\text{refl}} = P_c|F(\omega)|^2 + P_s\left\{|F(\omega+\Omega)|^2 + |F(\omega-\Omega)|^2\right\} \\
+ 2\sqrt{P_c P_s}\Big\{ \text{Re}\left[F(\omega)F^*(\omega+\Omega) - F^*(\omega)F(\omega-\Omega)\right]\cos(\Omega t) \\
+ \text{Im}\left[F(\omega)F^*(\omega+\Omega) - F^*(\omega)F(\omega-\Omega)\right]\sin(\Omega t)\Big\} + (2\Omega \text{ terms})
\end{aligned}
\tag{11}
$$

Within this expression, we are interested in the terms multiplied by the $\cos(\Omega t)$ and $\sin(\Omega t)$, as they contain information relevant to the carrier fields accumulated phase in the cavity.

From here, to extract the error signal, the signal measured at the reflection PD is then given to our Moku, where it is mixed at the EOM frequency of 20 MHz. This is due to the simple trig identity given by

$$
\sin(\Omega t)\sin(\Omega' t) = \frac{1}{2}\left\{\cos\left[(\Omega-\Omega')t\right] - \cos\left[(\Omega+\Omega')t\right]\right\} \tag{12}
$$

where we see that multiplying two sine functions yields two cosine terms. When the mixing signal frequency equals the EOM modulation frequency, one of the cosine terms becomes a DC term. A similar trig identity holds for mixing of the cosine term in Eq. 11. A phase offset is also utilized during this step to isolate either the cosine or sine term.

To extract this DC signal, the mixed signal is passed through a low pass filter we set to 10 MHz with the Moku. Finally, this isolates the term in Eq. (11) oscillating at $\Omega$, giving the PDH error signal

$$
\varepsilon = -2\sqrt{P_c P_s}\ \text{Im}\left\{F(\omega)F^*(\omega+\Omega) - F^*(\omega)F(\omega-\Omega)\right\} \tag{13}
$$

This error signal has the desirable quality in that it is antisymmetric about its zero crossing, making it suitable for feedback onto the cavity resonance. This error signal is then fed into a Proportional Integral Derivative (PID) feedback loop within the Moku where we seek to minimize the signal over time, keeping the cavity on resonance.

In a PID loop, feedback proportional to the current error is applied to direct the system towards resonance, while feedback that integrates over past errors seeks to minimize long term fluctuations. Finally, feedback that is a derivative of the error signal is utilized to minimize fast changes to the error signal. When optimizing our loop, each of these three terms had to be carefully balanced utilizing Moku's built in PID function.

Optimizing the PID loop to obtain a stable lock to the cavity took about a week. Once the lock had been established, we were able to take a Power Spectral Density (PSD) of both the error signal and the feedback signal generated by the PID loop to examine the lock's bandwidth and robustness, shown below in Fig. 3.

Two locks are compared in Fig. 3, due to a change in the beam profile caused by changing the fiber patch cable coupling the beam to free space that will be discussed in the challenges section.

The PSD of the feedback and error signals was measured for our PDH lock before and after replacing the fiber patch cable. We can see that the original lock setup achieved a unity-gain

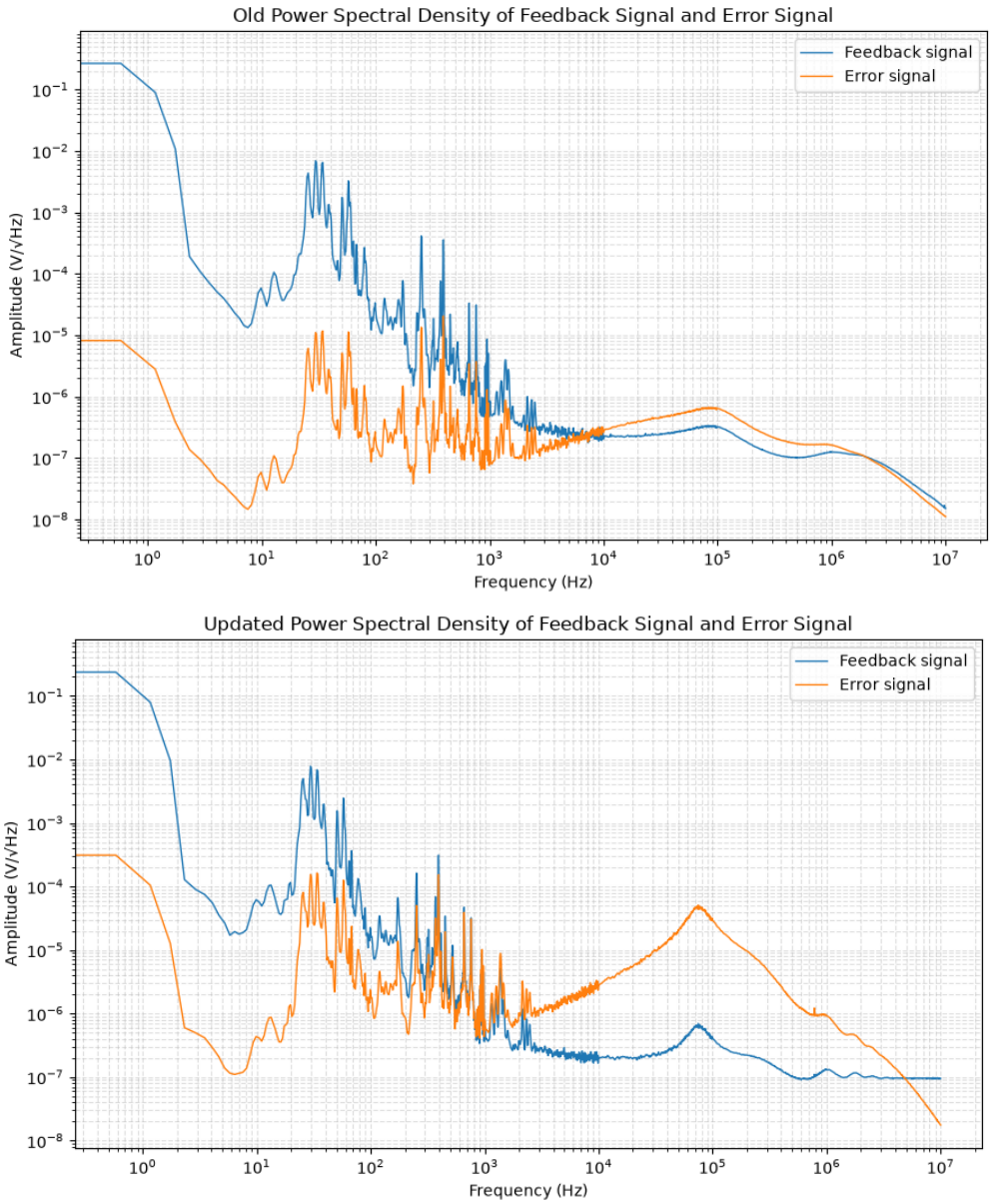



Figure 3: Top: The PSD of the first lock, with UGF of 10 KHz. Bottom: The PSD of the new lock obtained after switching the fiber patch cable, with UGF of 1 KHz.

frequency (UGF) of approximately 10 kHz, whereas the updated configuration exhibited a reduced UGF of approximately 1 kHz. The UGF represents the frequency up to where your control loop can provide feedback to the system, in other words, the bandwidth of the lock.

This order of magnitude reduction in loop bandwidth corresponds to degraded noise suppression up to the 10 kHz range in the new setup. In particular, we can see the new lock is about an order of magnitude noiser between 10 and 100 Hz as well. Finally, the new setup appears to have a new, significant noise source at 100 kHz, lying outside the setups current bandwidth. To improve the lock obtained, we will want to tune the PID loop settings until the error signal PSD is much lower in amplitude, resembling the previous setup or better.

### 5.2 Cavity Ring Down Measurement

With the cavity locked, we proceeded with performing a cavity ring down (CRD) measurement to find the finesse of the OEC. In a CRD measurement, the laser beam is rapidly extinguished, allowing light that has built up in the cavity to slowly leak out in an exponential decay. This exponential decay follows

$$P(t) = P_o e^{-t/\tau} \tag{14}$$

With $P_o$ the initial power, and $\tau = \frac{finesse*L}{\pi c}$. By fitting observed data to this exponential decay, the $\tau$ parameter can be determined giving a measure of the cavity finesse.

In our setup, to rapidly extinguish the beam we utilized a Mach-Zehnder (MZ) EOM. The max extinguishing ratio was found by stepping the minimum and maximum DC bias signal to minimize and maximize the measured power on the reflection PD. This maximum (4.05 V) and minimum (-0.40 V) bias was then input back into the MZ EOM as a square wave with a 0.1 Hz frequency and 20% duty cycle via a waveform generator. The cavity was then locked and the square wave output to the MZ EOM. Both the reflection PD and waveform generator outputs were sent to a 12 GHz oscilloscope, with a trigger set on the falling edge of the square wave to acquire the CRD waveform. The measured waveforms are shown below in Fig. 4.

Qualitatively, this appears how a CRD should look, with the power incident on the reflection PD exponentially decaying as the beam is rapidly extinguished. However, it was noticed that this same waveform was generated even when the cavity was not locked, when no intracavity field could build up. This points to the fact that we are not observing actual CRD, but rather the slow extinguishing of the beam by the MZ EOM.

To check this I setup a simple cavity ring down simulation utilizing python and the analytical reflected, intracavity, and transmitted fields given in Ref. [7], shown below in Fig. 5.

We can see that this shows that for our current cavity setup, with an estimade mode matching efficiency of 10%, it is better to perform the CRD measurement on the transmission PD, where the waveform is much clearer. A key next step, then, is to align our transmitted beam to a fast PD to view the exponential decay of the CRD measurement. We can then repeat the measurement, but this time utilizing the Moku's internal waveform generator, which should provide a faster signal to the MZ EOM avoiding the slow relaxation issue.

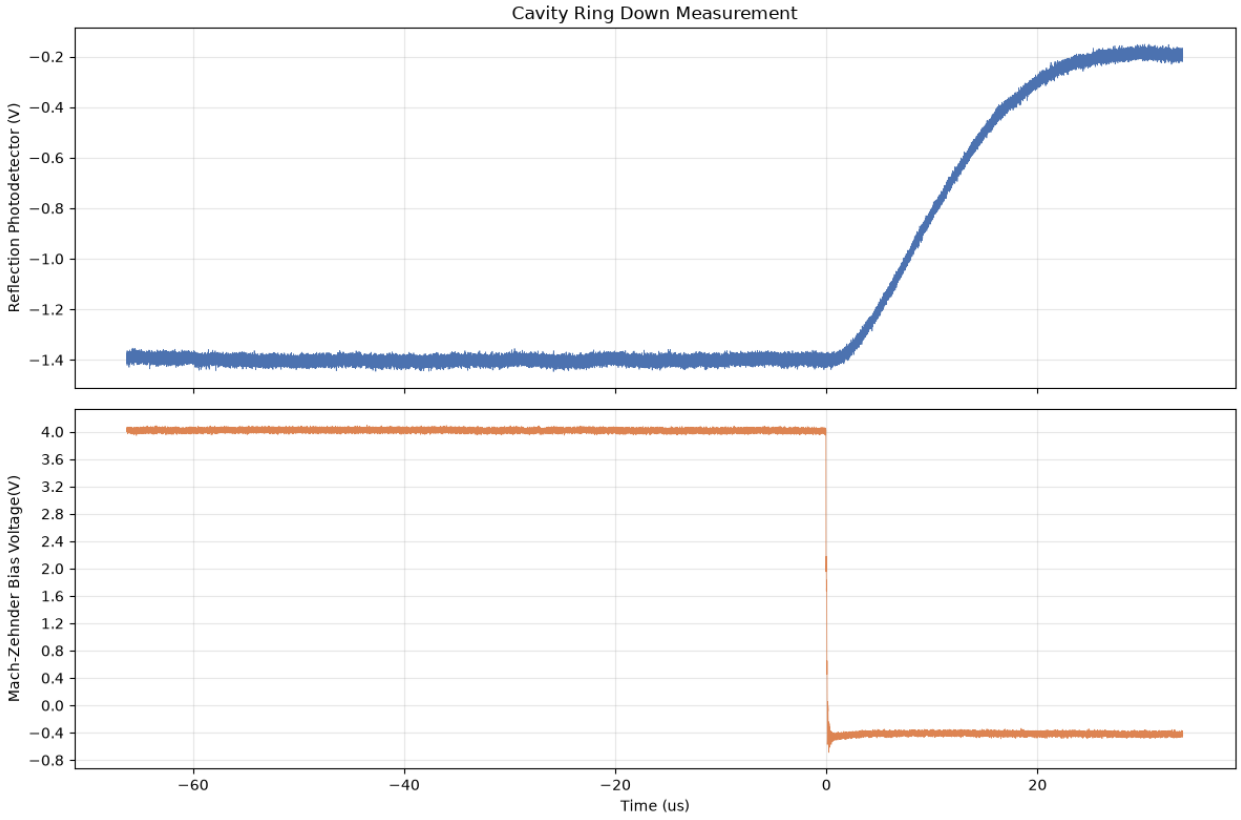



Figure 4: Cavity ring down results. Measured voltage on reflection PD (top) and MZ EOM input (bottom). Note, the reflection PD power is inverted due to the internal electronics of the PD.

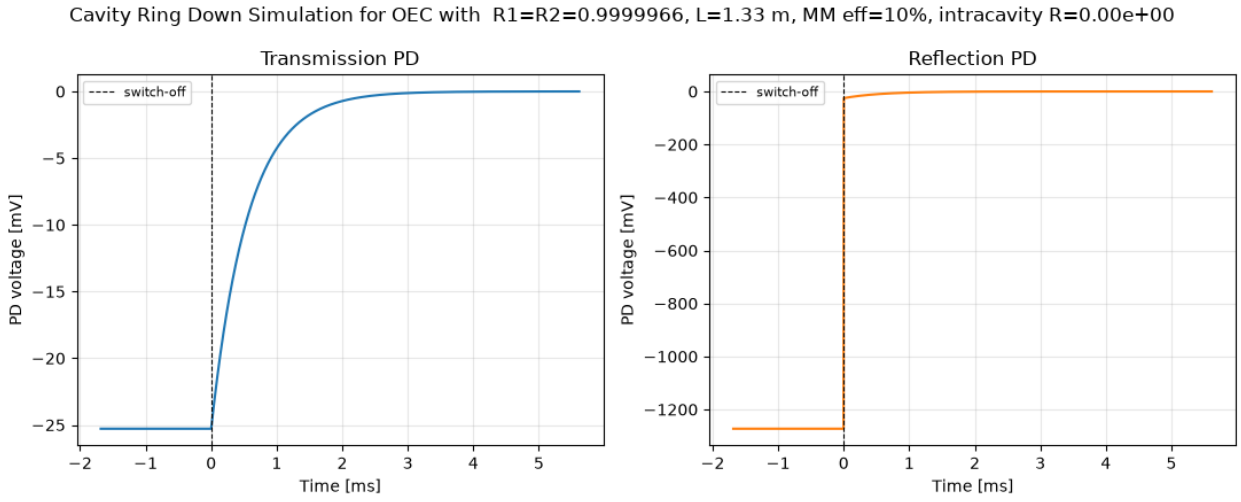



Figure 5: Simulation of expected cavity ring down curves on reflection and transmission photodetectors.

### 5.3 Challenges

A major challenge over the past month has been obtaining the first cavity lock. This was anticipated due to the narrow linewidth of the cavity, estimated at approximately 250 Hz, which is much smaller than the several kHz linewidth of our 1064 nm RIO laser system. This difference means that even when the laser is on resonance with the $TEM_{00}$ mode, only a small fraction of light enters into the cavity. Because the error signal in the PDH method is derived from the reflection dips observerd, which in turn is a function of how much light enters the cavity on resonance, our error signal was much smaller than desirable. More concretely, our measured error signal has been approximately 10 times less strong than expected of a critically coupled cavity.

Besides this challenge, we also encountered a setback once we did obtain a stable cavity lock. When adjusting optical components near the patch cable coupling our laser into free space, we noticed that any slight touches of the patch cable led to signficant changes in output power, at times up to 80% of our power. After investigating, we realized this was because the patch cable was not polarization maintaining (PM). Since it was not PM, any change to the orientation of the fiber changed the beams polarization, leading to a change in power after the beam passed through the polarizing beam splitter.

Because of this, we switched the patch cable to a new PM fiber. However, since a new fiber was utilized, the free space beam profile changed, making our past mode-matching and alignment work wrong.

This past week has been spent reprofiling the beam, and finding an updated mode matching solution, in the same manner as outlined in the Previous Work section. The updated solution consists of a f=250 mm lens at z=0.158m, and a lens of f=750 mm at z=0.364m. An upside to this is that in the new setup, we have improved mode matching into the cavity's eigenmode allowing for a greater percentage of power to enter into the cavity. Going forward, this will improve the power of the transmitted beam, which will make aligning to the transmission photodetector easier.

We were also able to obtain a new lock with much less effort than the previous time, pointing to better alignment and mode matching efficiency in this new setup. As pointed out in the discussion related to Fig. 3, however, we will need to improve upon the current feedback settings we are utilizing.

## 6 Future Steps

The immediate next step for this project are to optimize the PID loop utilized for locking the cavity. With the PID loop optimized, a larger feedback bandwidth should allow for a stronger lock and improved measurements of cavity parameters going forward.

Once this is done, another CRD measurement can be performed. To account for the slow extinguishing of the beam, the Moku's internal waveform generator will be utilized to extinguish the beam, rather than the Rigol waveform generator. With a successful measurement of the cavity finesse via the CRD measurement, we will proceed to do an FSR measurement of the cavity.

The primary goal for the rest of this project, however, is to analyze the characteristics of our laser pulses, and to perform pulse locking to the OEC. This primary goal of observing and performing pulse locking to the OEC has not changed throughout this project, as this is a novel step not yet examined by previous work on the OEC, and will inform future BLF work.

# References

[1] C. Cahillane and G. Mansell. *Review of the Advanced LIGO gravitational wave observatories leading to observing run four*. Galaxies, 10, 36 (2022). https://arxiv.org/pdf/2202.00847

[2] A. Sunahara, G. Raj, T. Cohen, P. M. Pattison, P. Rudy, Y. Ohara, S. Iizuka, H. Ohta, and S. Nakamura. *Laser-based inertial fusion energy system enabled by optical enhancement cavities and a direct-drive configuration reactor*. Opt. Express, 33, 47104–47120 (2025). https://opg.optica.org/oe/fulltext.cfm?uri=oe-33-22-47104

[3] T. Cohen, J. Mance, S. Gandrothula, K. Arai, F. S. Carcoba, H. Ohta, P. M. Pattison, P. Rudy, N. Svadlenak, C. Smith, R. Fukuda, S. Iizuka, Y. Ohara, K. Tsubakimoto, R. Adhikari, and S. Nakamura. *Recent progress for commercializing IFE based on a novel high efficiency 10 MJ laser and high gain fuel target*. Proc. SPIE, 13358, 13358-4 (2025). https://bluelaserfusion.com/wp-content/uploads/2025/07/BlueLaserFusion-SPIE-2025_Manuscript.pdf

[4] C. Bond, D. Brown, K. A. Strain, and A. Freise. *Interferometer techniques for gravitational-wave detection*. Living Rev. Relativ., 19, 3 (2016). https://arxiv.org/abs/0909.3661

[5] E. D. Black. *An introduction to Pound–Drever–Hall laser frequency stabilization*. Am. J. Phys., 69, 79–87 (2001).https://www.agpohl.physik.uni-mainz.de/files/2023/06/AmJPhys69_79_2001_Black_Intro_PDH.pdf

[6] Wikipedia contributors. *Pound–Drever–Hall technique*. Wikipedia, The Free Encyclopedia. https://en.wikipedia.org/wiki/Pound%E2%80%93Drever%E2%80%93Hall_technique.

[7] M. Weichman. *Simulating Cavity Transmission Spectra* (2023). https://weichman.princeton.edu/wp-content/uploads/2023/08/cavity_transmission_spectra.pdf

The proposal objectives and approach were also developed with help from Dr. Georgia Bolingbroke, Postdoctoral Scholar in Physics at Caltech